Journal of Integrative Neuroscience

J. Integr. Neurosci. **2026**; 25(11): 55300
https://doi.org/10.31083/JIN55300

Original Research

Social Isolation Aggravates Depression-like Behavior in Rotenone-Induced Parkinson's Disease Mice by Disrupting the Gut-Microbiota-Brain Axis

Yan Xu[1,2,†], Yuying Zhou[3,†], Yani Wang[4], Mingxuan Zheng[5,6], Xing Ge[5,7], Wei Pan[4,5], Kuiyang Zheng[4,5], Yinghua Yu[4,5], Deqin Geng[1,2,*]

[1]Graduate School, Nanjing Medical University, 211166 Nanjing, Jiangsu, China
[2]Department of Neurology, The Affiliated Hospital of Xuzhou Medical University, 221000 Xuzhou, Jiangsu, China
[3]Department of Gastroenterology, The Third Xiangya Hospital of Central South University, 410013 Changsha, Hunan, China
[4]Jiangsu Key Laboratory of Immunity and Metabolism, Xuzhou Medical University, 221004 Xuzhou, Jiangsu, China
[5]Department of Pathogen Biology and Immunology, School of Basic Medical Sciences, Xuzhou Medical University, 221004 Xuzhou, Jiangsu, China
[6]Department of Gastroenterology, Clinical Medical Research Center, The Suqian Clinical College of Xuzhou Medical University, 223800 Suqian, Jiangsu, China
[7]School of Public Health, Xuzhou Medical University, 221004 Xuzhou, Jiangsu, China
*Correspondence: gengdeqin@126.com (Deqin Geng)
[†]These authors contributed equally.
Academic Editors: Amedeo Amedei and Bettina Platt
Submitted: 25 June 2026 Revised: 3 August 2026 Accepted: 26 August 2026 Published: 17 November 2026

Abstract

Background: Parkinson's disease (PD) is a progressive neurodegenerative disorder with a rising global burden. Depression is one of the most common non-motor manifestations of PD and substantially worsens daily functions and disease prognosis. Social isolation (SI) is a common but underrecognized psychosocial stressor in PD patients due to motor impairments like resting tremor and abnormal gait; however, the mechanisms linking SI to depression aggravation are unclear. Considering the emerging role of the gut-microbiota-brain axis in PD development, intestinal homeostasis, neuroinflammation, and neuropsychiatric regulation, we investigated whether gut microbiota dysbiosis is implicated in depression-like behaviors aggravated by SI in a rotenone-induced mouse model of PD. **Methods:** A rotenone-induced PD mouse model was combined with SI. Depression-like behaviors, dopaminergic neuronal integrity, neurochemical alterations, serum corticosterone, intestinal inflammation, gut-barrier function, and gut microbial composition were assessed using behavioral tests, immunohistochemistry, biochemical assays, histological and molecular analyses, and 16S rRNA sequencing. Fecal microbiota transplantation (FMT) was conducted to examine whether microbiota from socially isolated PD mice could transfer related behavioral and pathological phenotypes to recipient mice. **Results:** SI significantly aggravated depression-like behaviors in rotenone-treated mice, along with further reduction in tyrosine hydroxylase-positive cells in the substantia nigra, lower hippocampal 5-hydroxytryptamine and brain-derived neurotrophic factor levels, and elevated serum corticosterone. SI also promoted intestinal inflammation and impaired gut-barrier integrity in PD mice. 16S rRNA sequencing demonstrated that SI reduced the alpha diversity of gut microbiota and altered microbial community composition. FMT from socially isolated PD mice reproduced depression-like behaviors, neurochemical abnormalities, and intestinal pathological alterations in the recipient mice, supporting the role of gut microbial dysbiosis in the aggravation of depression-like phenotypes by SI in PD. **Conclusions:** Our findings demonstrated that SI aggravates depression-like behaviors in rotenone-induced PD mice, at least partly through disruption of the gut-microbiota-brain axis. Regulation of intestinal microbiota may represent a potential approach for alleviating neuropsychiatric complications associated with PD.

Keywords: brain-gut axis; depression; fecal microbiota transplantation; gastrointestinal microbiome; Parkinson's disease; social isolation

1. Introduction

Parkinson's disease (PD) is the second most common neurodegenerative disease worldwide [1], and its prevalence is projected to increase substantially by 2050 [2], posing profound challenges to global health systems and patient well-being. Although PD is usually characterized by motor manifestations, non-motor symptoms are increasingly recognized as important contributors to disease burden [3]. Among them, depression is one of the most common and disabling neuropsychiatric symptoms, affecting approximately 38% of patients with PD and markedly impairing quality of life, functional independence, and disease prognosis [4]. Patients with PD are also prone to social isolation (SI) because of motor impairments, stigma, reduced social participation, and psychological distress. Clinical and experimental evidence has suggested that SI is associated with accelerated cognitive decline and worsened affective symptoms in PD [5]. However, the potential mech-

Copyright: © 2026 The Author(s). Published by IMR Press.
This is an open access article under the CC BY 4.0 license.

Publisher's Note: IMR Press stays neutral with regard to jurisdictional claims in published maps and institutional affiliations.

anisms through which SI exacerbates depression in PD are poorly understood, which limits the advancement of targeted strategies for patients in socially vulnerable groups.

The microbiota-gut-brain axis has emerged as a fundamental pathway linking gastrointestinal homeostasis, immune regulation, and brain function [6]. Recent evidence has indicated that gut microbiota dysbiosis contributes to PD pathogenesis and progression by modulating neuroinflammation, oxidative stress, intestinal-barrier integrity, and neurotransmitter metabolism [7]. Chronic psychosocial stress can also reshape the gut microbial ecosystem and influence affective behaviors. Previous studies have reported associations between stress-related behavioral phenotypes and alterations in specific bacterial taxa, including *Eubacterium*, *Anaerofustis*, and *Lactobacillus* [8,9,10]. Those findings raise the possibility that SI may worsen PD-associated depression phenotypes by disrupting gut microbiota composition and intestinal-barrier function. However, whether gut microbiota alterations contribute to depression-like behaviors aggravated by social isolation under pathological conditions associated with PD has been insufficiently investigated.

Here, we combined a rotenone-induced PD mouse model with solitary housing to model SI in the context of PD pathology. We tested for comprehensive depression-like behaviors, gut histopathological and molecular analyses, and 16S rRNA-based microbiota profiling. Furthermore, we conducted fecal microbiota transplantation in order to examine whether intestinal microbiota from socially isolated PD mice could reproduce related behavioral and pathological phenotypes in recipient mice. Our study aimed to clarify whether gut microbial dysbiosis is involved in the aggravation of depression-like behaviors by social isolation in PD, and to provide experimental evidence supporting the microbiota-gut-brain axis as a candidate target for alleviating neuropsychiatric complications associated with PD.

2. Methods

2.1 Animals

Seven-week-old male C57BL/6J mice (weighing 20–23 g) were purchased from the Beijing Vital River Laboratory Animal Technology Co., Ltd. (Beijing, China) and kept in the Experimental Animal Center of Xuzhou Medical University. They were allowed free access to food and water. All mice were maintained in a specific pathogen-free, temperature-controlled room kept at 24 °C under a 12-hour day/night cycle. All animal care and experimental procedures were in strict accordance with the Laboratory Animal Welfare and Ethics Committee (LAWEC) of Xuzhou Medical University (Xuzhou, China; Approval No. 202309T002). The study was conducted in accordance with the ARRIVE 2.0 guidelines, and the completed ARRIVE checklist is provided in **Supplementary Table 1**.

2.2 Experimental Design

After a one-week acclimatization period, the mice were stratified by body weight and randomly allocated to four experimental groups (n = 15 per group): (1) Group-housed mice (5/cage) received oral gavage saline as the control group (CON); (2) Individually-housed mice received oral gavage saline as the SI group; (3) Group-housed mice administered rotenone (10 mg/kg/day, cat. no. R8875, Sigma-Aldrich, St. Louis, MO, USA) by oral gavage for 4 consecutive weeks according to previously established and behaviorally validated protocol as the PD group (PD) [11,12]; (4) Individually-housed mice administered rotenone for 4 consecutive weeks as the PD + SI group (PD + SI). Social isolation was induced by housing each mouse individually in a separate cage for 4 consecutive weeks, thereby preventing direct physical interaction with conspecifics. All mice underwent the behavioral tests of open field test (OFT), sucrose preference test (SPT), tail suspension test (TST), after which, mice were euthanized with pentobarbital sodium (P3761, Sigma-Aldrich, St. Louis, MO, USA) (100 mg/kg body weight) via intraperitoneal injection. Brain samples, blood, colon, and cecal contents were then harvested and stored at –80 °C for further analysis (**Supplementary Fig. 1**). Animals used for each downstream analysis were randomly selected from each group.

2.3 Fecal Microbiota Transplantation (FMT)

Fecal microbiota transplantation (FMT) was conducted to explore the role of intestinal microbiota in SI-aggravated depression in PD mice. The FMT experiment initially included 60 recipient mice, with 15 mice allocated to each of the four recipient groups. First, antibiotics, including neomycin sulfate (1 g/L, A610366, Sangon Biotech, Shanghai, China), metronidazole (1 g/L, A600633, Sangon Biotech, Shanghai, China), ampicillin sodium (1 g/L, A610028, Sangon Biotech, Shanghai, China), and vancomycin hydrochloride (0.25 g/L, A600983, Sangon Biotech, Shanghai, China) were administered to recipient mice to deplete the indigenous gut microbiota before FMT: (1) mice receiving microbiota from CON mice were the Fecal microbiota transplantation from control mice (FMT^{CON}) group; (2) mice receiving microbiota from SI mice were the Fecal microbiota transplantation from social isolation mice (FMT^{SI}) group; (3) mice receiving microbiota from the PD group were the Fecal microbiota transplantation from Parkinson's disease mice (FMT^{PD}) group; (4) mice receiving microbiota from PD + SI mice were the Fecal microbiota transplantation from Parkinson's disease + social isolation mice (FMT^{PD+SI}) group.

In detail, these recipient mice first received a 2-week broad-spectrum antibiotic pretreatment via drinking water, containing neomycin (1 g/L), metronidazole (1 g/L), ampicillin (1 g/L), and vancomycin (0.25 g/L) [13]. The protocol of FMT was performed according to established meth-

ods [14,15,16]. Briefly, fresh fecal samples from donor mice in clean cages were collected daily into sterile tubes. Roughly 100 mg of feces (equivalent to 5–6 pellets) was immediately transferred to ice-chilled sterile tubes to maintain microbial viability. Subsequently, fecal samples were mixed thoroughly in cold phosphate-buffered saline (PBS; G4202-500ML, Servicebio, Wuhan, Hubei, China) at a 100 mg/1000 µL ratio, followed by a 15-min incubation. The homogenate was passed through a 70-µm cell strainer (352350, Corning, Corning, NY, USA) to collect the filtrate. After centrifugation at 4 °C for 5 min to retrieve the bacterial suspension, it was diluted with an equivalent volume of PBS to assess the optimal FMT concentration (approximately 10^{11} CFU/L). Prepared suspensions were administered once daily to recipient mice (10 mL/kg) via oral gavage. After a 1-week post-FMT period to allow for microbial colonization, behavioral tests were conducted [17]. These mice were then euthanized with pentobarbital sodium, and brain samples, blood, colon, and colon contents were then harvested and stored at –80 °C for analysis (**Supplementary Fig. 2**).

2.4 Behavioral Testing

Depression-like behaviors were assessed using OFT, SPT, TST, and following well-established protocols [18,19,20,21]. All mice underwent the same behavioral test battery in a predetermined order (OFT, SPT, and TST). Both behavioral assessments and data analyses were conducted by investigators blinded to group allocation.

The SPT protocol consisted of three phases: (1) Adaptation (48-h exposure to 1% sucrose and regular water provided with two separate drinking bottles in home cages with *ad libitum* food), (2) Baseline measurement (12-h access to both solutions in test chambers), and (3) Preference testing (24-h deprivation followed by 12-h access to both solutions during dark phase). The sucrose preference index (%) is calculated as: [sucrose consumption (g) / (sucrose consumption + water consumption)] × 100%. Rodents with emotional deficits typically exhibit decreased sucrose preference, presumably resulting from diminished responsiveness to rewarding stimuli [22,23].

The TST is a behavioral assay conducted to assess a depression-like phenotype in rodents. After habituation to controlled laboratory conditions for 24 h before the trial phase, mice were suspended head-down by the tail from a horizontal bar at 20–25 cm height against a plain background. The 6-min trial begins with a 1-min adaptation phase (excluded from analysis due to acute stress responses), followed by 5 min of automated immobility-time recording (in seconds) using the SMART 3.0 video tracking system (Panlab SL, Barcelona, Spain). Mice typically exhibit initial agitation followed by gradual immobility, a state designated as “behavioral despair” [19]. The tail was secured close to the body to minimize tail-climbing behavior during the test. Total immobility time was used as the primary TST outcome.

OFT evaluates spontaneous locomotion, exploratory behavior, and anxiety-like responses in rodents exposed to novel environments. After 5 min of adaptation to the trial environment 24 h before the trial phase, mice were placed facing away from the experimenter in the central zone (36 × 36 cm). Automated tracking software, SMART 3.0 video tracking system (Panlab SL, Barcelona, Spain), quantifies vertical exploratory activity and total distance of spontaneous locomotion over a 10-min session.

2.5 Immunohistochemistry

Immunohistochemical analyses were conducted on 20-µm serial frozen brain sections. Briefly, to suppress endogenous peroxidase activity, the sections were exposed to 0.3% H_2O_2 (0.3%, G0115, Servicebio, Wuhan, Hubei, China) for 15 min. After three 5-min rinses in PBS, the sections were permeabilized with 0.3% Triton X-100 (0.3%, X100, Sigma-Aldrich, St. Louis, MO, USA) for an additional 15 min. After three additional washes with PBS, the sections were blocked with 5% goat serum (5%, G9023, Sigma-Aldrich, St. Louis, MO, USA) for 1 h at room temperature, then incubated with primary antibodies (tyrosine hydroxylase (TH) antibody: 1:500, sc-25269, Santa Cruz Biotechnology, Dallas, TX, USA) overnight at 4 °C. The next day, the sections underwent three PBS washes before being incubated with goat anti-mouse secondary antibody (1:1000, SA00001-1, Proteintech, Rosemont, IL, USA) at room temperature for 2 h. TH-immunoreactive cells were quantified within the anatomically defined substantia nigra pars compacta were quantified by using an optical fractionator method with Stereo Investigator software (version 7, MBF Bioscience, Williston, VT, USA) under an Olympus BX52 microscope (Olympus America Inc., Melville, NY, USA).

2.6 Western Blot Analysis

The hippocampus was rapidly dissected from the brain on ice, snap-frozen in liquid nitrogen, and stored at −80 °C until protein and RNA extraction. Ice-cold radioimmunoprecipitation assay (RIPA) lysis buffer (20-188, Millipore, Burlington, MA, USA) supplemented with complete ethylenediaminetetraacetic acid (EDTA)-free protease inhibitor cocktail and phosphatase inhibitor components (P1046, Beyotime Biotechnology, Shanghai, China) was used to extract proteins from homogenized hippocampal tissue [24,25]. Protein concentration was quantified using the bicinchoninic acid (BCA) protein assay kit (Beyotime Biotechnology, Shanghai, China, Cat# P0010). Then, equivalent amounts of protein were resolved by sodium dodecyl sulfate-polyacrylamide gel electrophoresis (SDS-PAGE) (08091, Sigma-Aldrich, St. Louis, MO, USA) and subsequently transferred onto polyvinylidene difluoride membranes (Millipore, Burlington, MA, USA, Cat#

ISEQ00010). Subsequently, the membranes were first treated with 5% skim milk (5%, M7409, Sigma-Aldrich, St. Louis, MO, USA) prepared in Tris-buffered saline with Tween 20 (TBST) buffer (G0004-500ML, Servicebio, Wuhan, Hubei, China) at room temperature and were then incubated with the corresponding primary antibodies at 4 °C for 12 h: anti-β-actin (AC004, ABclonal, Wuhan, China, 1:10,000), anti-brain-derived neurotrophic factor (BDNF) (SJ12-09, Huabio, Hangzhou, China, 1:5000). Afterward, the membranes were washed 3 times in TBST buffer and probed with horseradish peroxidase (HRP)-conjugated anti-mouse immunoglobulin G (IgG) secondary antibody (AS003, ABclonal, Wuhan, China, 1:5000) or HRP-conjugated anti-rabbit IgG secondary antibody (AS014, ABclonal, Wuhan, China, 1:5000) for 1 h. Finally, chemiluminescent signals were developed using Clarity™ enhanced chemiluminescence (ECL) Western Blotting Substrate (1705060, Bio-Rad, Hercules, CA, USA) and subsequently visualized and recorded with a ChemiDoc Touch Imaging System (1708370, Bio-Rad, Hercules, CA, USA).

2.7 Quantitative Reverse Transcription Polymerase Chain Reaction (qPCR)

Total RNA was isolated from colon and hippocampal tissue samples using a previously established method [26,27]. Briefly, homogenized tissues were processed with Trizol reagent (15596026, Thermo Fisher Scientific, Inc., Waltham, MA, USA) under sterile conditions for total RNA extraction. Subsequently, cDNA was generated from 1 µg of total RNA with a High-Capacity cDNA Reverse Transcription Kit (R223-01, Vazyme Biotech Co., Ltd., Nanjing, China), followed by qPCR analysis on a LightCycler® 480 II Real-time PCR Instrument (05015278001, Roche, Basel, Switzerland). qPCR was conducted using the SYBR Green Master Mix (RR820A, Takara Bio, Kusatsu, Shiga, Japan) according to the manufacturer's protocol. The relative mRNA expression levels of tumor necrosis factor-α (TNF-α), interleukin-1β (IL-1β), and interleukin-6 (IL-6) were evaluated using the comparative CT method ($2^{-\Delta\Delta Ct}$). The primer sequences used are listed as follows: mIL-1β forward (F): TGGGAAACAACAGTGGTCAGG; mIL-1β reverse (R): CTGCTCATTCACGAAAAGGGA; mIL-6 forward (F): TCACAGAAGGAGTGGCTAAGGACC; mIL-6 reverse (R): ACGCACTAGGTTTGCCGAGTAGAT; mTNF-α forward (F): CTTGTTGCCTCCTCTTTTGCTTA; mTNF-α reverse (R): CTTTATTTCTCTCAATGACCCGTAG; mβ-actin forward (F): GGCTGTATTCCCCTCCATCG; mβ-actin reverse (R): CCAGTTGGTAACAATGCCATGT.

2.8 Immunofluorescence

Colon zonula occludens-1 (ZO-1) and occludin were used to assess the gut-barrier integrity as previously reported [14,28]. Colon tissue samples were immersed in 4% paraformaldehyde (4%, G1101, Servicebio, Wuhan, Hubei, China) for fixation. After a 30-min blocking step with 3% bovine serum albumin (BSA; 3%, G5001, Servicebio, Wuhan, Hubei, China) at room temperature, the colon tissue sections were incubated with the primary antibodies (ZO-1 antibody: Servicebio, GB11195, 1:200 dilution; occludin antibody: MCE, HY-P81155, 1:100 dilution) at 4 ℃ overnight. After PBS washing, the sections were incubated for 2 h with a Cy3-conjugated goat anti-rabbit secondary antibody (Servicebio, GB21303; 1:300). Nuclear counterstaining was performed with 4′,6-diamidino-2-phenylindole (DAPI) (Servicebio, G1012), and fluorescence images were subsequently acquired using an Olympus IX51 fluorescence microscope (Olympus, Tokyo, Japan).

2.9 Thickness Measurements of the Colon Mucus Layer

The thickness of the colon mucus layer was measured by Alcian blue staining as previously described [29]. The colon samples after Carnoy's fixation (G1120-500ML, Servicebio, Wuhan, Hubei, China) underwent paraffin embedding, were sectioned into 5-µm sections, and mounted on glass slides. After deparaffinization and hydration, Alcian blue (pH 2.5, ab150662, Abcam, Cambridge, UK) staining was performed for 30 min, after which the sections were washed, dehydrated, cleared in xylene, and cover-slipped. The stained slides were then used to acquire thousands of partially overlapping images along nearly the entire colon for morphometric analysis. The thickness of the mucus layers was quantified using ImageJ (version 1.54f, National Institutes of Health, Bethesda, MD, USA).

2.10 Enzyme-Linked Immunosorbent Assay (ELISA)

The 5-hydroxytryptamine (5-HT) concentration in the hippocampal tissue samples and serum corticosterone (CORT) were detected using the Mouse 5-HT Kit (AF2443-A, AiFang Biological, Changsha, Hunan, China) and the Mouse CORT ELISA Kit (AF2061-A, AiFang Biological, Changsha, Hunan, China) according to the manufacturer's protocol [30]. A spectrophotometer (ClinBio128, Asys Hitech GmbH, Eugendorf, Austria) was used to determine the absorbance at 545 nm (Asuragen ClinBio128, USA). The measurement of 5-HT was conducted in duplicate for all samples.

2.11 Gut Microbiota Analysis

Cecal contents were obtained and preserved at –80 °C for further analysis. Microbial DNA was extracted from cecal content using the E.Z.N.A. stool DNA Kit (D4015, Omega Bio-tek, Norcross, GA, USA). PCR amplification targeted the V3-V4 hypervariable region of the bacterial 16S rRNA gene using barcoded 341F and 806R primers. PCR reactions were amplified in three parallel reactions with KOD polymerase (KOD-201, TOYOBO, Osaka, Japan). The thermal cycling protocol included an initial denaturation at 98 °C for 1 min, followed by 30 cy-

cles of denaturation at 98 °C for 10 s, annealing at 50 °C for 30 s, and extension at 72 °C for 30 s, with a final extension at 72 °C for 5 min. Amplicons were purified, quantified, and pooled in equimolar ratios. Sequencing libraries were prepared according to standard Illumina protocols and sequenced on the NovaSeq 6000 system (Illumina, San Diego, CA, USA) using an SP flow cell with a 2 × 250 bp paired-end configuration at Majorbio Bio-Pharm Technology Co., Ltd. (Shanghai, China). Sequence reads underwent quality control and chimera screening before being grouped into operational taxonomic units (OTUs) at 97% sequence similarity using the UPARSE pipeline (version 7.1; https://www.drive5.com/uparse/). Taxonomic identities were subsequently assigned with reference to the SILVA database(SSU release 115; https://www.arb-silva.de/) [31].

2.12 Fecal Water Content Detection

Mice were individually kept in clean cages with free access to food and water after a 24-h fasting period, as previously described [32]. Fecal samples were collected immediately upon excretion over a 12-h interval from 0800 h to 2000 h, and their morphology was recorded. The total wet weight of all collected samples was measured. Subsequently, the samples were dried in a 56 °C oven for 48 h to determine their dry weight. The fecal water content was calculated as (wet weight–dry weight) / wet weight × 100%.

2.13 Statistical Analysis

Data were expressed as mean ± Standard Error of the Mean (SEM). Statistical analyses were conducted using GraphPad Prism 8.0 (GraphPad Software, San Diego, CA, USA), and the distribution of continuous variables was evaluated for normality with the Shapiro-Wilk test. Two-way ANOVA was used to assess the main effects of rotenone treatment and social isolation and their interaction, followed by Tukey's multiple-comparison test for pairwise comparisons among the four groups. In the FMT experiments, one-way ANOVA followed by the Tukey–Kramer test was used to compare the four recipient groups. Alpha-diversity indices were analyzed using two-way ANOVA, followed by Tukey's multiple-comparisons test for all six pairwise comparisons among the four experimental groups (**Supplementary Table 2**). Principal coordinate analysis (PCoA) was used to visualize variation in gut microbial community structure, and overall differences among the four experimental groups (CON, SI, PD, and PDSI) were assessed using analysis of similarities (ANOSIM) based on Bray–Curtis dissimilarity with 999 permutations. LEfSe analysis was performed to identify differentially abundant bacterial taxa using the Kruskal–Wallis rank-sum test, followed by the Wilcoxon rank-sum test to assess consistency across subclasses when applicable, and linear discriminant analysis (LDA) to estimate effect sizes. The significance thresholds for LEfSe were $p < 0.05$ and |LDA score| >2. No Benjamini–Hochberg false discovery rate (BH-FDR) correction was applied within the LEfSe analysis, and no separate Wilcoxon-based differential abundance analysis with BH-FDR correction was performed for microbial taxa. Spearman's correlation analysis was conducted using 24 paired observations pooled from the four experimental groups (six paired observations per group) to examine the relationship between specific gut microbiota and behavior test results. No multiple-comparison correction was applied to the Spearman correlation analyses; therefore, the reported p-values are unadjusted (**Supplementary Table 3**). These correlations were interpreted as exploratory findings and should be interpreted with caution because pooling samples across the four experimental groups may introduce between-group heterogeneity. Accordingly, the observed correlations may partly reflect differences among the experimental groups rather than within-group associations. For analyses other than the exploratory Spearman correlation analyses, $p \leq 0.05$ was considered statistically significant.

Sequence processing and statistical analysis of the 16S rRNA data were performed on the Majorbio Cloud Platform (https://www.majorbio.com/).

3. Results

3.1 Social Isolation Worsened Depression-Like Behaviors and Neurochemical Alterations in Rotenone-Induced PD Mice

To validate the rotenone-induced PD-like phenotype, we assessed spontaneous locomotor activity using the total distance traveled in the open field test. Rotenone-treated mice showed a significantly lower total distance traveled than saline-treated mice (**Supplementary Fig. 3A**), indicating reduced spontaneous locomotor activity. Together with the significant reduction in substantia nigra TH-positive cells (Fig. 1D,E), this finding supports the induction of a PD-like phenotype in the present cohort.

SI has been reported to induce detrimental effects on depression in PD patients [33]. However, evidence in animal models is limited. To clarify the impact of SI on PD-related depression, we used an individually housed PD mouse model and performed a series of behavioral and neurochemical assays. Compared with group-housed PD mice, socially isolated PD mice exhibited a significantly lower sucrose preference index (Fig. 1A), a longer duration of immobility during the tail suspension test (Fig. 1B), and exhibited lower vertical-activity counts in the open field test (Fig. 1C). Terminal body weight did not differ significantly among the CON, SI, PD, and PD + SI groups (all $p > 0.05$; **Supplementary Fig. 4A**). SI exacerbated these depression-like behaviors in control mice. These behavioral results suggested that social isolation aggravated depression-like behaviors in rotenone-induced PD mice.

We next examined whether SI affected dopaminergic neuronal loss in the substantia nigra. Immunohistochemical staining showed fewer TH-positive cells in the substantia

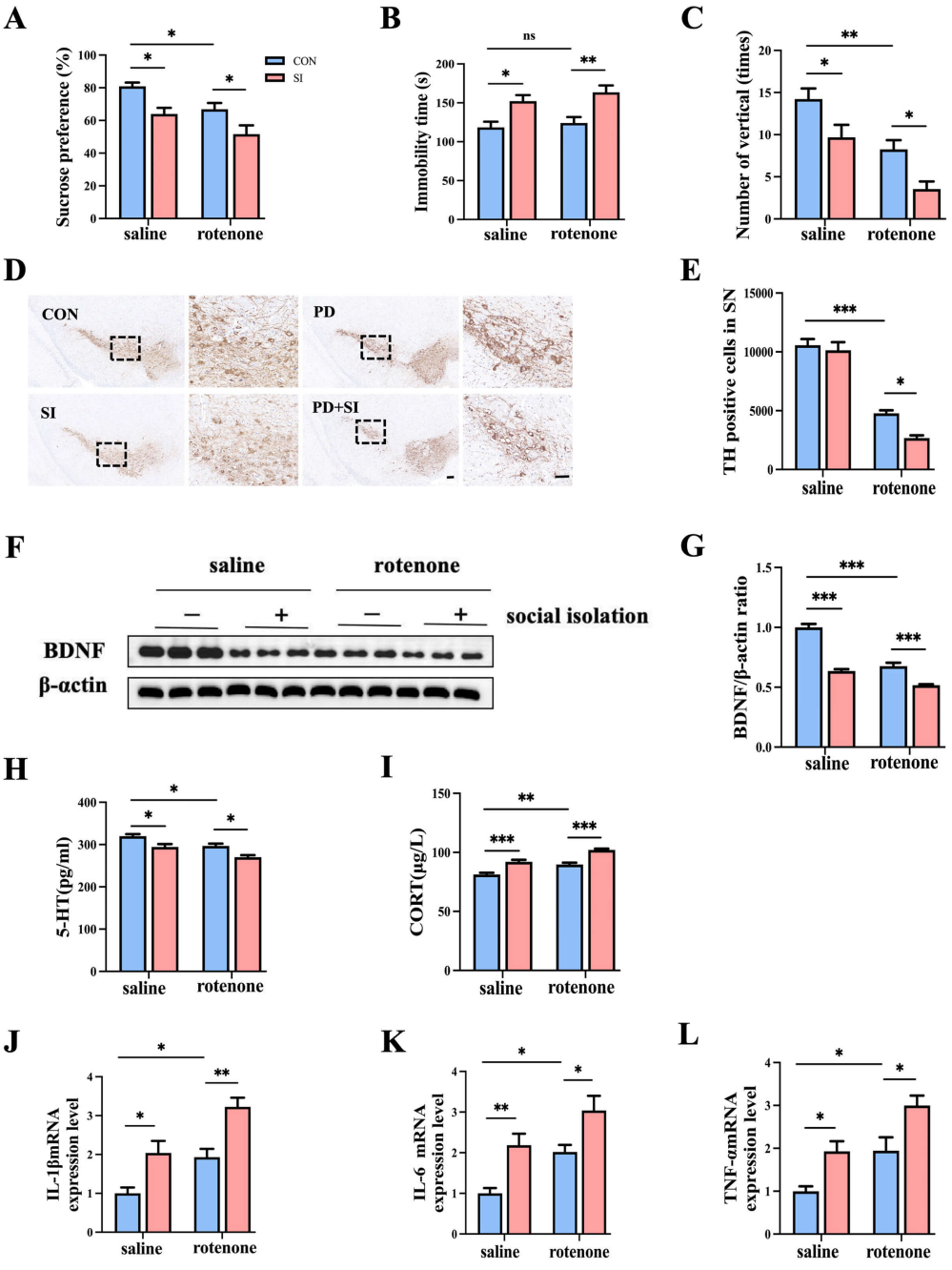


Fig. 1. Social isolation worsens depression-like behaviors and neurochemical changes in rotenone-induced Parkinson's disease (PD) mice. (A) Sucrose preference test (SPT) (n = 15/gp). (B) Duration of immobility during the tail suspension test (TST) (n = 15/gp). (C) Number of vertical explorations in the open field test (OFT) (*n* = 15/gp). (D) Representative images showing tyrosine hydroxylase (TH)-positive cells in the substantia nigra. Scale bar: 50 μm. (E) Quantitative assessment of TH-positive cells in the substantia nigra (*n* = 3/gp). (F) Representative Western blot images showing brain-derived neurotrophic factor (BDNF) expression in the hippocampus. (G) Quantitative analysis of hippocampal BDNF protein expression relative to β-actin (*n* = 6/gp). Full-length blots corresponding to Fig. 1F are presented in the original WB images. (H) 5-hydroxytryptamine (5-HT) levels in hippocampus (*n* = 7/gp). (I) Serum corticosterone (CORT) level (*n* = 7/gp). (J–L) qPCR assessment of IL-1β, IL-6, and TNF-α mRNA expression in hippocampal tissue (*n* = 6/gp). Values are expressed as mean ± SEM. Two-way ANOVA was used to assess the main effects of rotenone treatment and social isolation and their interaction, followed by Tukey's multiple-comparison test for pairwise comparisons among the four groups. ns, not significant ($p > 0.05$); * $p < 0.05$; ** $p < 0.01$; *** $p < 0.001$. Con, Control; SI, Social isolation; IL-1β, interleukin-1β; IL-6, interleukin-6; TNF-α, tumor necrosis factor-α; SEM, standard error of the mean.

nigra with rotenone treatment, and this difference appeared more pronounced in PD + SI mice (Fig. 1D,E). These findings suggested that SI exacerbated dopaminergic neuronal damage under PD pathological conditions. At the neurochemical level, social isolation was associated with significantly lower hippocampal 5-HT and BDNF levels and higher serum CORT levels in rotenone-treated mice (Fig. 1F–I). At the neuroinflammatory level, SI mice showed higher hippocampal mRNA levels of IL-1β, IL-6, and TNF-α (Fig. 1J–L). These alterations are consistent with enhanced anhedonia, a heightened stress response, and impaired neuroplasticity [34].

3.2 Social Isolation Exacerbated Intestinal Inflammation and Gut-Barrier Dysfunction in Rotenone-Induced PD Mice

Given the critical involvement of the gut-brain axis in PD pathophysiology [35], we next investigated whether SI affected intestinal homeostasis in rotenone-induced PD mice. Compared with group-housed mice, SI mice showed significantly shorter colon lengths in both saline-treated controls and rotenone-treated PD mice, with the shortest colon length observed in the PD + SI group (Fig. 2A,B). Consistently, socially isolated PD mice had significantly higher colonic mRNA levels of IL-1β, IL-6, and TNF-α than group-housed PD mice (Fig. 2C–E). Rotenone treatment was also associated with lower fecal water content; however, SI mice did not show further altered fecal water content with or without rotenone treatment (Fig. 2F). These results suggested that SI enhanced intestinal inflammatory responses in PD mice without markedly affecting fecal water content.

We then assessed intestinal-barrier integrity, a key factor in gut-brain communication [28]. Alcian blue staining showed that SI mice had a thinner colon inner mucus layer in both control and PD mice (Fig. 2G,H). Immunofluorescence staining further revealed significantly lower positive area fractions of ZO-1 and occludin in socially isolated mice than in the corresponding group-housed mice under both saline-treated and rotenone-treated conditions (Fig. 2I–L). Together, these data indicated that SI aggravated intestinal inflammation and disrupted both the colon mucus barrier and epithelial tight-junction integrity in rotenone-induced PD mice.

3.3 Social Isolation Aggravated Gut Microbiota Dysbiosis and Reshaped Microbial Community Composition in Rotenone-Induced PD Mice

Given the close relationship between intestinal health and brain function [36], we profiled the cecal microbiota using 16S rRNA gene sequencing, and found that SI mice showed significantly lower abundance-based coverage estimator index (ACE), Chao1, and Sobs indices (Sobs represent observed OTU richness, whereas Chao1 and ACE estimate microbial richness, with higher values indicating greater richness) in both saline-treated and rotenone-treated mice, indicating less microbial richness in mice subjected to SI (Fig. 3A–C). Principal coordinates analysis (PCoA) of OTU-based community demonstrated clear separation of the microbial communities across the four groups, suggesting that both rotenone treatment and SI markedly reshaped the overall gut microbiota structure (Fig. 3D). At the taxonomic level of phylum, SI mice showed greater levels of *Patescibacteria* in PD mice (Fig. 3E). At the genus level, SI was associated with a higher level of *Lactobacillus* and lower levels of the *Lachnospiraceae NK4A136* group and *norank f norank o Clostridia UCG-014* (Fig. 3F). Linear discriminant analysis effect size (LEfSe) revealed a characteristic microbial profile in PD mice, characterized by enrichment of *class Clostridia*, *order Oscillospirales*, *family Ruminococcaceae*, *genus Eubacterium siraeum group*, and *family Oscillospiraceae*. Notably, the *order Eubacteriales*, *family Anaerofustaceae*, *genus Anaerofustis*, and *genus Eubacterium ventriosum group* were the highest enriched in the PD + SI group (Fig. 3G). Additional LEfSe comparisons showed that SI, PD, and PD + SI mice each exhibited taxa that were distinct from control mice, further supporting the presence of treatment-specific microbial signatures (**Supplementary Fig. 5**). Moreover, direct comparison between PD and PD + SI mice revealed SI-associated microbial alterations under PD conditions, strengthening the evidence that SI aggravated disruption of the gut-microbial community in a rotenone-induced mouse model of PD.

Spearman's correlation analysis further linked specific taxa with behavioral outcomes (Fig. 3H). The findings indicated that the *genus Lactobacillus* was inversely correlated with the sucrose preference index, whereas the *genus norank of family Muribaculaceae* was positively correlated. Moreover, the abundance of the *genus Lachnospiraceae NK4A136 group* showed an inverse correlation with immobility time in the tail suspension test. Regarding anxiety-like behavior, the abundances of the *genera Turicibacter*, *Allobaculum*, and *Ileibacterium* showed positive correlations with the number of vertical explorations in the open field test. In contrast, the abundance of the *genus norank of the family Lachnospiraceae* was negatively correlated with this measure. Collectively, these findings suggested that SI aggravated gut microbial alterations in a rotenone-induced mouse model of PD and that specific microbial taxa are associated with depression-like behavioral alterations.

3.4 FMT From Socially Isolated Rotenone-Induced PD Mice Recapitulated Depression-Like Behaviors and Produced Neurochemical Abnormalities in Recipient Mice

To determine whether gut microbiota alterations contributed to SI-induced depression-like phenotypes in PD mice, FMT was performed using fecal samples from control mice, SI mice, PD mice, and PD + SI mice. Recipient mice that received microbiota from PD mice showed less sucrose preference, and this difference was even greater in mice receiving fecal microbiota from PD + SI mice (Fig.

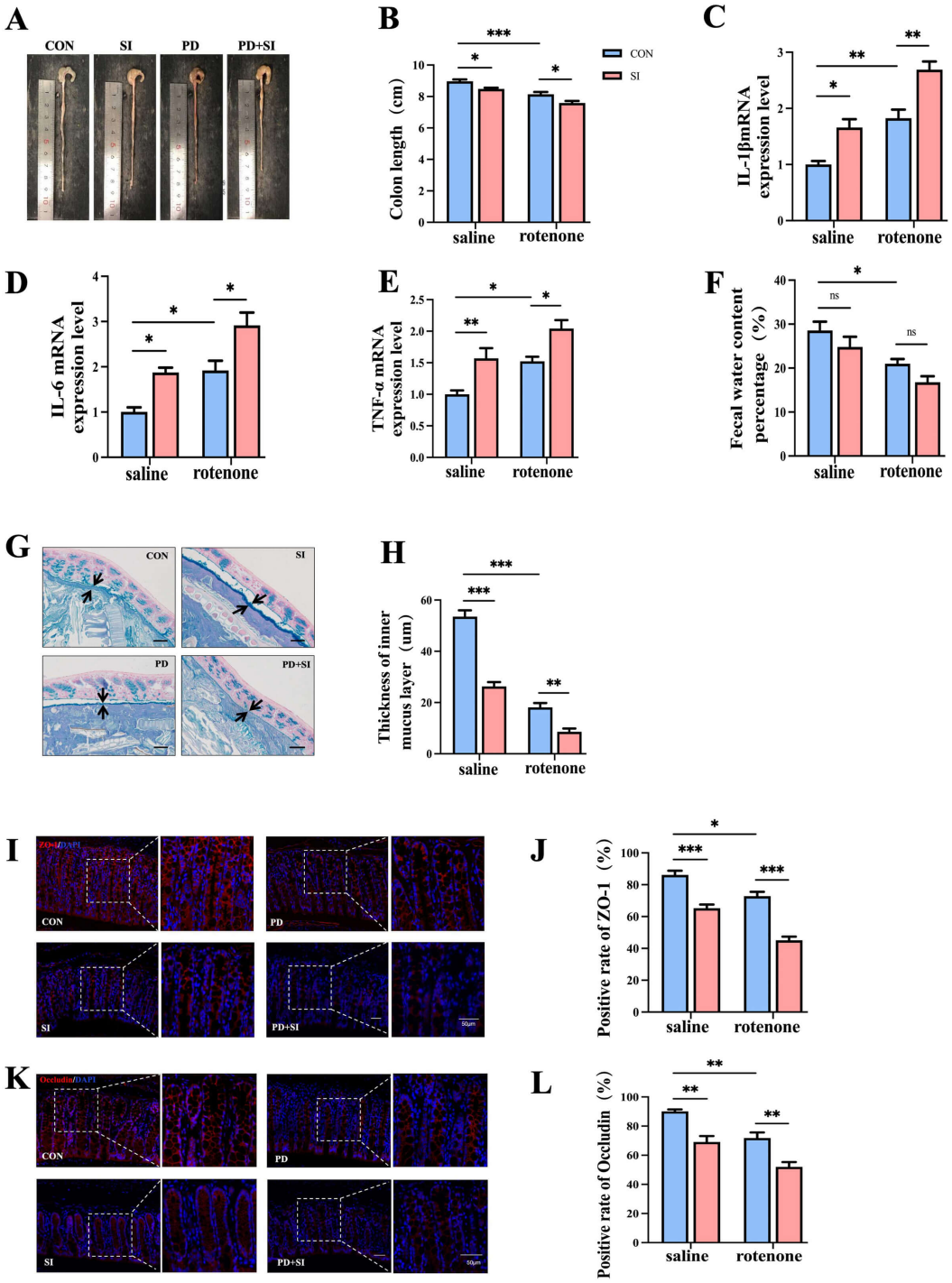


Fig. 2. Social isolation exacerbates intestinal inflammation and gut barrier dysfunction in rotenone-induced PD mice. (A) Representative images of the colon. (B) The colon length (n = 9/gp). (C–E) Colon mRNA levels of IL-1β, IL-6, and TNF-α (n = 6/gp). (F) Fecal water content percentage (n = 9/gp). (G) The representative images of Alcian blue staining. The thickness of the mucus layer is marked by opposing black arrows. Scale bar: 50 μm. (H) Quantitative analysis of the inner mucus layer thickness (n = 5/gp). (I) Representative fluorescence images of colon sections stained for ZO-1. Scale bar: 50 μm. (J) Quantitative analysis of ZO-1 positive area fraction (n = 3/gp). (K) Representative immunofluorescence images of colon sections stained for occludin. Scale bar: 50 μm. (L) Quantitative analysis of occludin positive area fraction (n = 3/gp). Values are expressed as the mean ± SEM. Two-way ANOVA was used to assess the main effects of rotenone treatment and social isolation and their interaction, followed by Tukey's multiple-comparison test for pairwise comparisons among the four groups. ns, not significant ($p > 0.05$); * $p < 0.05$; ** $p < 0.01$; *** $p < 0.001$. ZO-1, zonula occludens-1.

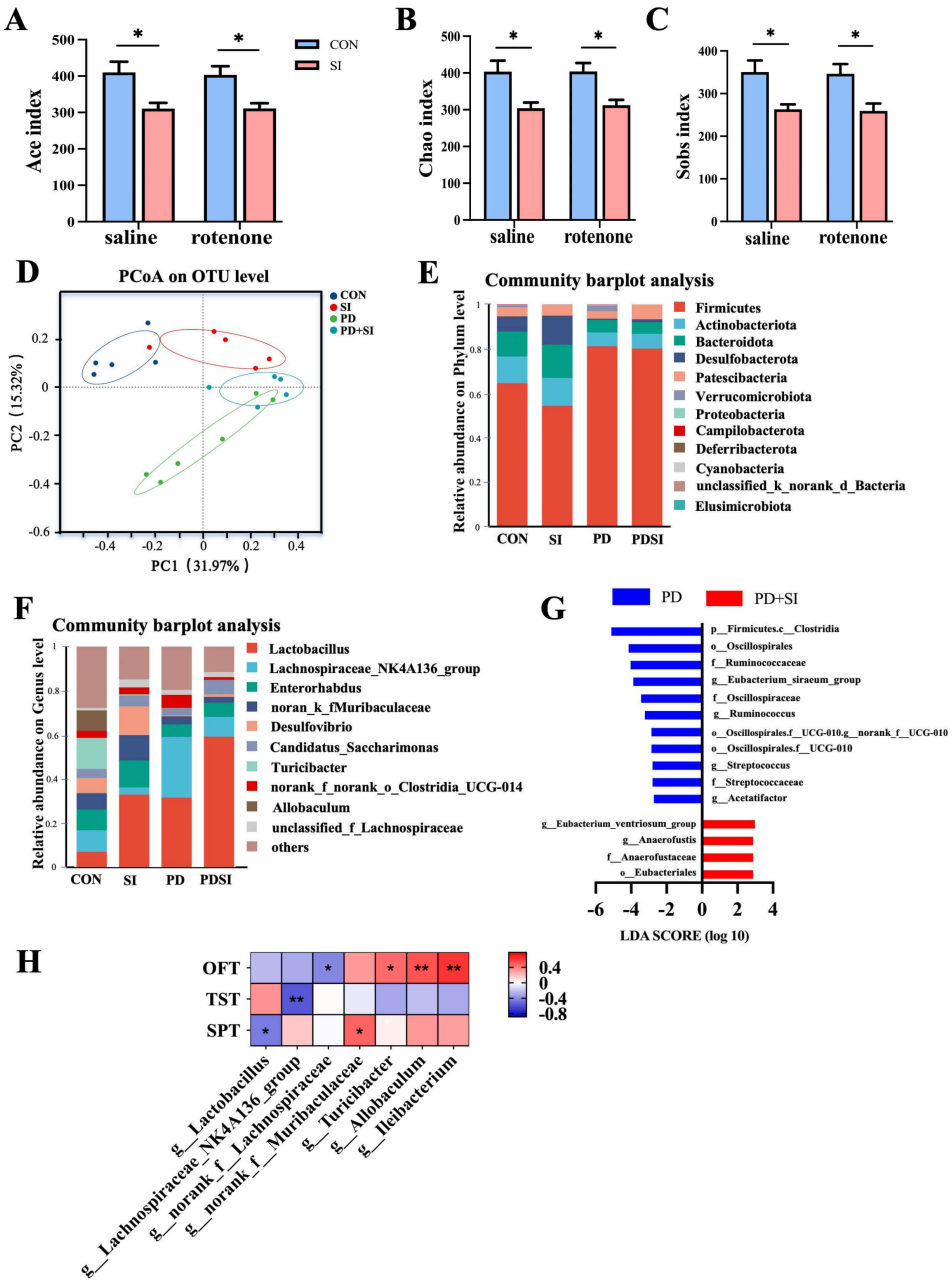


Fig. 3. Social isolation aggravates gut microbiota dysbiosis and reshapes microbial community composition in rotenone-induced PD mice. (A–C) Alpha-diversity indices (Ace, Chao1, and Sobs) of gut microbiota. Two-way ANOVA was used to assess the main effects of rotenone treatment and social isolation and their interaction, followed by Tukey's multiple-comparison test for pairwise comparisons among the four groups. (D) Principal coordinates analysis (PCoA) profiling of the gut microbial community at the operational taxonomic unit level based on unweighted UniFrac distances. Overall differences in gut microbial community structure among the four experimental groups were assessed using analysis of similarities (ANOSIM; R = 0.4037, p = 0.001). (E) Phylum-level relative abundance of the predominant bacterial taxa. (F) Relative abundances of the predominant bacterial genera. (G) Linear discriminant analysis effect size (LEfSe) identifying taxa with differential abundance between the PD and PD + SI groups. Blue bars indicate taxa enriched in the PD group, and red bars indicate taxa enriched in the PD + SI group. Taxa meeting the criteria of a linear discriminant analysis |(LDA) score| >2 and $p < 0.05$ are displayed. (H) Spearman correlation heatmap showing the associations between selected bacterial taxa and behavioral outcomes in the open field test, tail suspension test, and sucrose preference test. Correlations were calculated using pooled data from all four groups (24 paired observations; six per group). Red and blue indicate positive and negative correlations, respectively. n = 6/gp, values are expressed as the mean ± SEM. * $p < 0.05$; ** $p < 0.01$. SI, Social isolation; PD, Parkinson's disease; PD + SI, Parkinson's disease with social isolation; OFT, Open field test; TST, Tail suspension test; SPT, Sucrose preference test.

4A). Body weight measured before sacrifice did not differ significantly among the four FMT groups (all $p > 0.05$; **Supplementary Fig. 4B**). Similarly, FMT from PD + SI mice was further associated with greater duration of immobility during the tail suspension test (Fig. 4B), as well as a shorter total travel distance (**Supplementary Fig. 3B**) and less vertical exploration (Fig. 4C), compared with the FMT from PD mice. Immunohistochemical analysis showed that recipient mice that received fecal microbiota from PD + SI mice exhibited a lower number of TH-positive cells than did those receiving fecal microbiota from PD mice (Fig. 4D,E). These behavioral and neuropathological alterations were accompanied by lower hippocampal BDNF and 5-HT levels, along with higher serum CORT (Fig. 4F–I) and higher hippocampal mRNA levels of IL-1β, IL-6, and TNF-α (Fig. 4J–L). Collectively, the FMT findings support a contributory role for gut microbiota dysbiosis in the SI-associated exacerbation of depression-like behaviors and neurochemical dysfunction in PD mice.

3.5 FMT From Socially Isolated Rotenone-Induced PD Mice Transferred Intestinal Inflammation and Barrier Damage to Recipient Mice

To evaluate whether gut microbiota contributed to SI-induced gastrointestinal abnormalities, we performed FMT in antibiotic-pretreated wild-type recipient mice. Recipients transplanted with microbiota from SI-exposed donors exhibited marked gastrointestinal alterations. FMT^{SI} mice showed significantly shorter colon lengths than did FMT^{CON} mice, and this effect was further evident when FMT^{PD+SI} mice were compared to FMT^{PD} mice (Fig. 5A,B). Consistently, colon mRNA levels of IL-1β, IL-6, and TNF-α were higher in recipients receiving microbiota from SI donors, with the highest levels observed in the FMT^{PD+SI} group (Fig. 5C–E). Fecal water content was lower only in recipients of microbiota from PD mice (Fig. 5F).

We next assessed whether the transferred microbiota also impaired intestinal-barrier integrity. Alcian blue staining showed that recipients of microbiota from SI-exposed donors had a significantly thinner inner colon mucus layer, particularly in the FMT^{PD+SI} group (Fig. 5G,H). Immunofluorescence staining further revealed lower positive area fractions of ZO-1 and occludin in the colonic epithelium of FMT^{SI} and FMT^{PD+SI} mice (Fig. 5I–L). These results demonstrated that SI-associated gut pathology can be transferred via the microbiota.

4. Discussion

Previous clinical evidence has shown that SI adversely affects both depressive symptoms and physiological function in PD patients [33]. However, the underlying mechanisms were unclear. In the present study, we provided experimental evidence that SI exacerbates depression-like behaviors in rotenone-induced PD mice, in addition to dopaminergic neuronal loss, neurochemical abnormalities, hippocampal neuroinflammation, intestinal inflammation, gut-barrier impairment, and gut microbiota dysbiosis. Moreover, FMT from socially isolated PD mice reproduced these pathological and behavioral phenotypes in recipient mice, supporting the role of gut-microbiota dysbiosis in the aggravation of depression-like phenotypes by SI under Parkinsonian conditions.

SI is a prevalent but frequently neglected psychosocial burden in PD patients [5]. Consistent with previous clinical and preclinical evidence [5,37], we found that SI exacerbated depression-like behaviors in rotenone-induced PD mice, which manifested as lower sucrose preference, prolonged immobility in the tail suspension test, and decreased vertical exploration in the open field test. These behavioral measures are thought to correspond respectively to anhedonia, "behavioral despair", and diminished exploratory motivation, which are commonly used indicators of depression-like states in rodents. Furthermore, SI was associated with fewer TH^+ cells in the substantia nigra, lower levels of hippocampal 5-HT and BDNF, and higher CORT in PD mice, providing neurochemical evidence for the aggravated depression-like state. These findings suggest that the exacerbation of affective disturbances by SI in PD is associated with stress-related alterations in monoaminergic signaling, neurotrophic support, and hypothalamic-pituitary-adrenal axis activation. This interpretation is consistent with evidence that prolonged psychological stress can engage hypothalamic-pituitary-adrenal signaling and peripheral and central inflammatory pathways, with downstream effects on hippocampal function and BDNF-related plasticity [38]. These results aligned with clinical observations that loneliness and social withdrawal in patients with PD are associated with more severe non-motor symptoms and poorer quality of life [5].

The intestinal microenvironment, particularly in regard to the interaction between gut microbiota and host immunity, has been increasingly implicated in depression and PD-related neuropsychiatric dysfunction [7]. We showed that SI aggravated intestinal pathological changes in PD mice, evidenced by shorter colon length and higher levels of pro-inflammatory cytokines. Also, SI compromised gut-barrier function, including a thinner mucus layer and lower positive area fractions of ZO-1 and occludin. These findings indicated that SI may further compromise intestinal homeostasis in the context of PD. It is interesting to note that these pathological alterations were closely associated with alterations of gut-microbiota composition: SI was significantly associated with reduced alpha diversity and altered the relative abundance of several bacterial genera, including enrichment of stress-susceptible taxa such as *Anaerofustis* and the *Eubacterium ventriosum* group [8,9]. At the genus level, *Lactobacillus* was more abundant in PD + SI mice. Notably, although *Lactobacillus* is often regarded as beneficial, its functional role can vary accord-

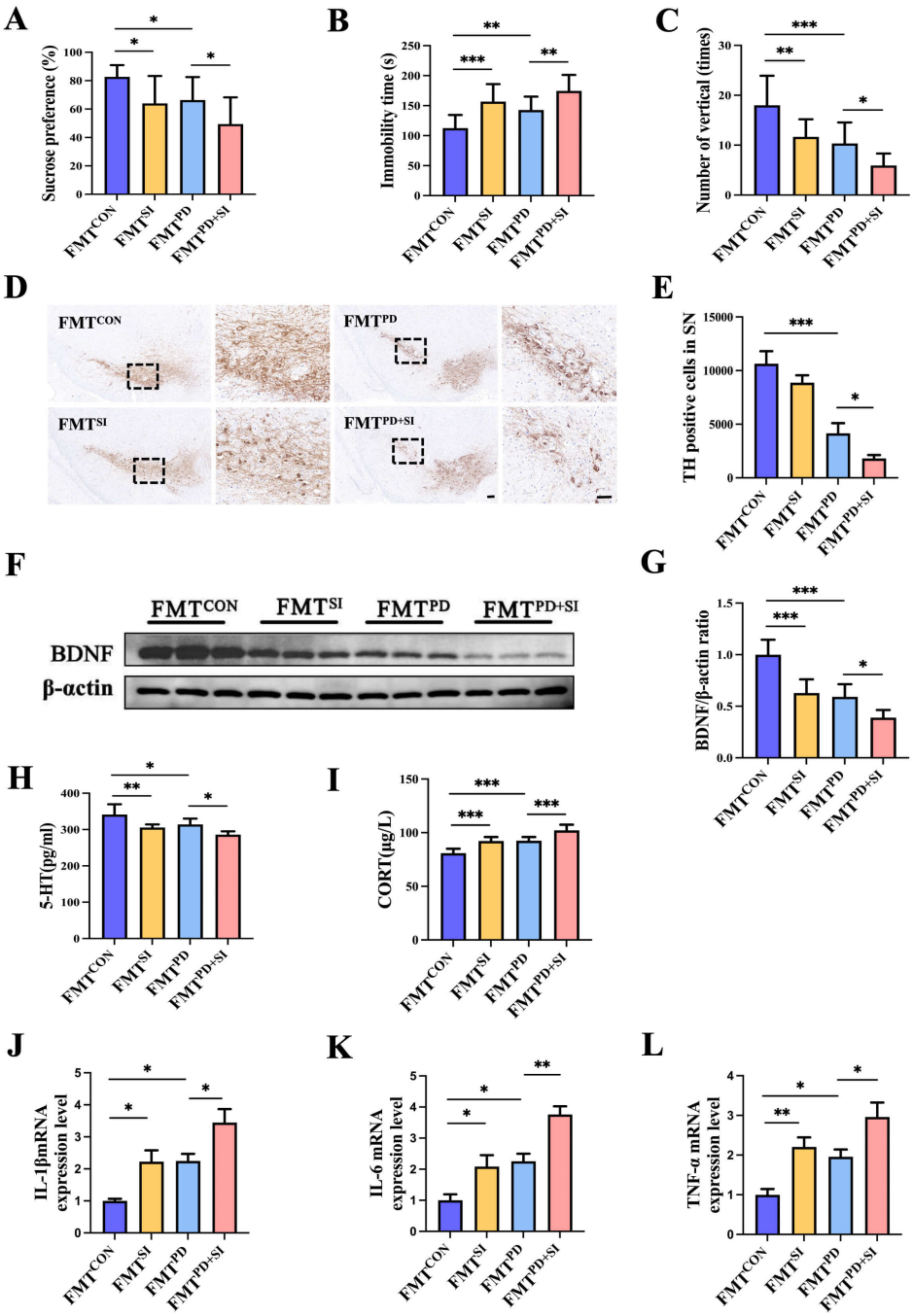


Fig. 4. FMT from socially isolated rotenone-induced PD mice recapitulated depression-like behaviors and neurochemical abnormalities in recipient mice. (A) SPT (n = 15/gp). (B) Duration of immobility during the TST (n = 15/gp). (C) Number of vertical explorations in the OFT (*n* = 15/gp). (D) Representative immunohistochemical staining images of TH-positive cells within the substantia nigra. Scale bar: 50 μm. (E) Quantitative assessment of TH-positive cells in the substantia nigra (*n* = 3/gp). (F,G) Representative Western blot images and quantitative analysis of hippocampal BDNF protein expression (*n* = 6/gp). Full-length blots corresponding to Fig. 4F are presented in the original WB images. (H) Hippocampal 5-HT concentration (*n* = 7/gp). (I) Serum corticosterone (CORT) level (*n* = 7/gp). (J–L) qPCR-based assessment of IL-1β, IL-6, and TNF-α transcript levels in hippocampal tissue. Values are expressed as the mean ± SEM. The four FMT recipient groups were compared using one-way ANOVA followed by the Tukey–Kramer multiple-comparison test. * $p < 0.05$; ** $p < 0.01$; *** $p < 0.001$. Con, Control; SI, Social isolation; PD, Parkinson's disease; FMT^{Con}, Fecal microbiota transplantation from control mice; FMT^{SI}, Fecal microbiota transplantation from social isolation mice; FMT^{PD}, Fecal microbiota transplantation from Parkinson's disease mice; FMT^{PD+SI}, Fecal microbiota transplantation from Parkinson's disease + social isolation mice.

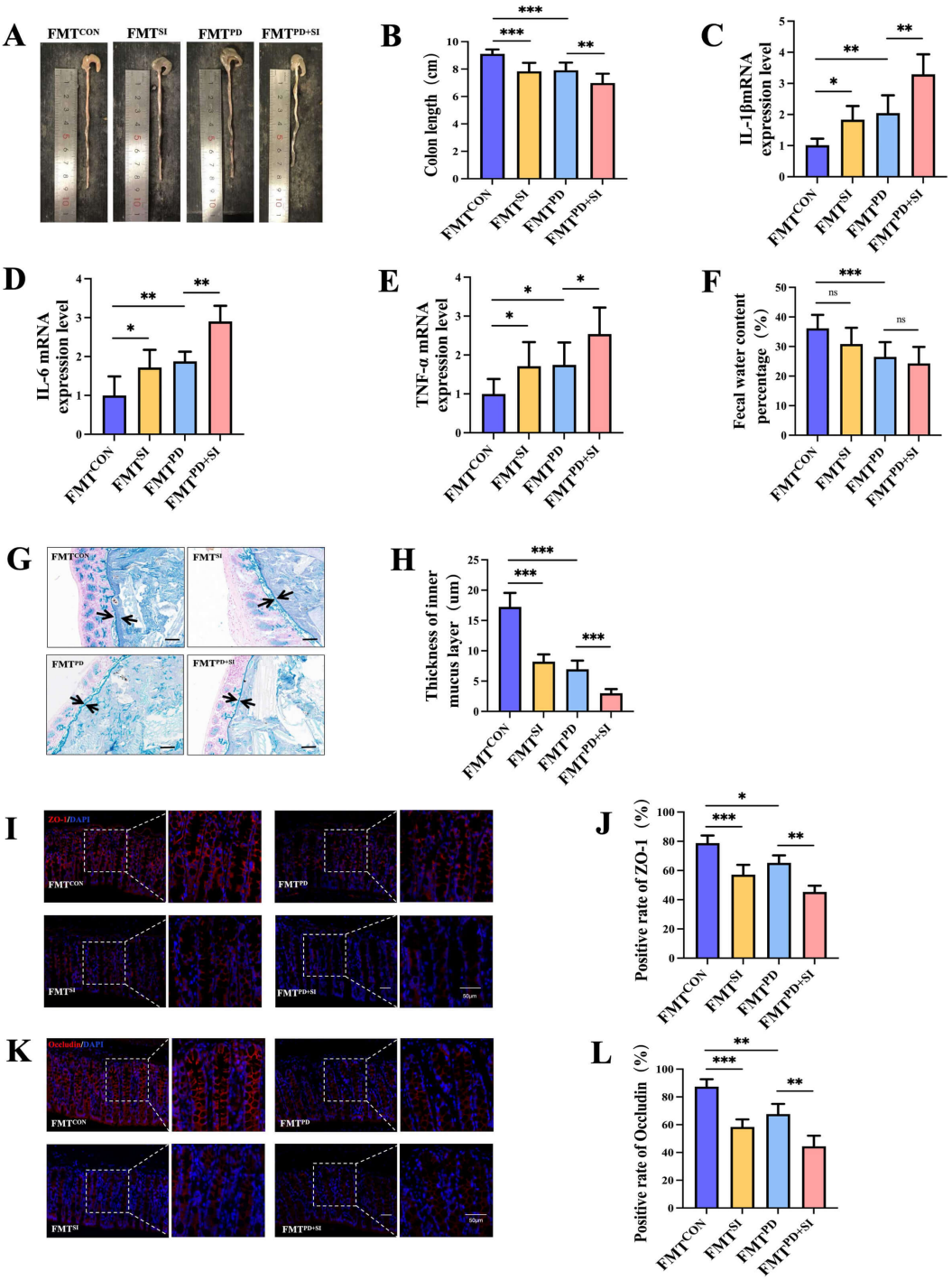


Fig. 5. FMT from socially isolated rotenone-induced PD mice transfers intestinal inflammation and barrier damage to recipient mice. (A) Representative images of colons. (B) Colon length (n = 9/gp). (C–E) Quantification of mRNA levels of IL-1β, IL-6, and TNF-α in colon tissue by qPCR (n = 6/gp). (F) Fecal water content percentage (n = 9/gp). (G) Representative images of Alcian blue staining. The thickness of the mucus layer is marked by opposing black arrows. Scale bar: 50 μm. (H) Quantification of the inner mucus layer thickness (n = 5/gp). (I) Representative fluorescence images of colon sections stained for ZO-1. Scale bar: 50 μm. (J) Quantitative analysis of ZO-1 positive area fraction (n = 3/gp). (K) Representative immunofluorescence images of colon sections stained for occludin. Scale bar: 50 μm. (L) Quantitative analysis of occludin positive area fraction (n = 3/gp). Values are expressed as the mean ± SEM. The four FMT recipient groups were compared using one-way ANOVA followed by the Tukey–Kramer multiple-comparison test. ns, not significant ($p > 0.05$); * $p < 0.05$; ** $p < 0.01$; *** $p < 0.001$.

ing to the host pathological state, microbial community structure, and metabolic activity. In certain clinical PD cohorts, increased *Lactobacillus* abundance has been associated with altered disease features and intestinal levodopa metabolism [39]. Therefore, the effects of specific bacterial taxa should be interpreted in relation to the host pathological state, microbial community structure, and metabolic activity rather than being classified as universally beneficial or harmful. Accordingly, SI may shift the gut microbiota toward a dysbiotic configuration that promotes intestinal inflammation and barrier dysfunction. Intestinal pathology may also intersect with PD-specific protein pathology, as fatty acid-binding protein 2 (FABP2) has been implicated in α-synuclein uptake by enteric neurons [40]. Impaired intestinal-barrier integrity may represent an important interface linking gut microbiota dysbiosis to brain dysfunction. In line with this hypothesis, we observed higher hippocampal mRNA levels of IL-1β, IL-6, and TNF-α, together with reduced BDNF and 5-HT levels, in PD + SI mice. Consistent with a broader interaction between neuroinflammatory activity and dopaminergic integrity, a previous 1-methyl-4-phenyl-1,2,3,6-tetrahydropyridine (MPTP) mouse study demonstrated that L-3,4-dihydroxyphenylalanine (L-DOPA)-mediated inhibition of NOD-like receptor family pyrin domain-containing 3 (NLRP3) inflammasome activation paralleled elevated TH levels in the substantia nigra and striatum, alongside ameliorated motor behaviors [41]. These changes provide a plausible mechanistic link between intestinal pathology and depression-like behaviors in PD.

The gut microbial alterations observed in this study were partly consistent with those reported in previous PD studies. Increased *Lactobacillus/Lactobacillaceae* and reduced *Lachnospiraceae* and other short-chain fatty acid (SCFA)-producing bacteria have been frequently reported in PD cohorts and meta-analyses [42,43,44], broadly aligning with the increased *Lactobacillus* and decreased *Lachnospiraceae NK4A136* group observed here. Similar community-level alterations have also been described in rotenone-based PD models [45,46]. However, microbiota findings in PD remain heterogeneous, and no universally reproducible taxonomic signature has been established across populations and experimental models [42,43,44,47,48]. In the present study, the microbial differences between PD+SI and PD mice therefore likely represent SI-associated remodeling superimposed on rotenone-related dysbiosis, rather than a direct recapitulation of the gut microbiota profile of idiopathic PD.

To further examine whether gut microbiota contributed to the SI-associated aggravation of depression-like behaviors in PD, we performed FMT. Transplantation of microbiota from PD + SI donors into antibiotic-pretreated recipients reproduced the behavioral, neurochemical, intestinal inflammatory, and barrier abnormalities observed in donor mice, supporting a transferable contribution of altered gut microbial communities. Notably, FMT from PD donors also reduced the number of tyrosine hydroxylase (TH-positive) cells in the substantia nigra, with a further reduction following FMT from PD + SI donors. Because recipient mice were not themselves administered rotenone, this graded pattern supports a microbiota-associated contribution to nigral dopaminergic alterations, with SI further amplifying the effect. Potential mechanisms include intestinal-barrier dysfunction and increased systemic exposure to microbial products such as lipopolysaccharide (LPS), which may activate Toll-like receptor 4 (TLR4)-related inflammatory and neuroimmune responses that compromise dopaminergic integrity [12,34]. Microbiota-derived metabolites may also influence neuroimmune and neurochemical pathways [7]. However, rotenone-induced TH-positive cell loss has been observed in both germ-free and conventionally raised mice, whereas motor dysfunction and barrier impairment were more microbiota-dependent [45]. Thus, altered gut microbial communities likely act as transferable modifiers and amplifiers, rather than the sole cause, of nigral pathology. Because FMT co-transfers microbial communities and associated products, and these mediators were not directly assessed here, their specific contributions remain unresolved. Correlation analyses provided additional clues regarding microbial taxa that may be involved in behavioral regulation. Certain bacterial genera (e.g., *Muribaculaceae*) have been negatively correlated with depressive-like behaviors [49], whereas others such as *Turicibacter* and *Allobaculum* were associated with lowered anxiety-like behaviors [50,51,52], further supporting the potential of specific microbial communities to modulate emotional homeostasis. Collectively, these associations supported the possibility that SI can disturb emotional homeostasis by enriching stress-susceptible or inflammation-associated bacteria and reducing potentially beneficial microbial communities. However, correlation does not establish causality. Future studies using targeted bacterial supplementation, metabolomic profiling, and microbial depletion or reconstruction strategies are required to define the precise microbial drivers of social isolation-aggravated depression in PD.

From a translational perspective, our findings suggested that SI is a possible modifiable risk factor for neuropsychiatric deterioration in PD. These results supported the importance of routine psychosocial assessment, early identification of loneliness, and promotion of social engagement as part of comprehensive PD management. In addition, the microbiota-gut-brain axis may represent an intervention target for patients with PD who are vulnerable to depression and SI. Furthermore, SI is not a PD-specific stressor and may engage general stress-responsive neuroendocrine, immune, and microbial pathways [53]. However, our findings suggest that these effects are amplified in a PD-like pathological context. Compared with PD mice, PD + SI

mice exhibited more pronounced behavioral, neurochemical, intestinal, and dopaminergic abnormalities. Moreover, FMT from PD + SI donors produced more severe abnormalities than FMT from PD donors, supporting a transferable microbiota-associated component of this exacerbation. These findings suggest that social isolation may act as a context-dependent amplifier of PD-associated depressive and intestinal phenotypes rather than through a mechanism unique to PD.

Limitations

This study had several limitations. First, the mechanisms underlying rotenone-associated gut microbiota alterations remain unresolved. These changes may reflect both direct intestinal exposure and indirect host-mediated effects related to oxidative stress, inflammation, barrier dysfunction, and gastrointestinal disturbances [45,46]. The observation that intraperitoneal rotenone can also alter gut microbial composition [54] further suggests that direct luminal exposure alone is unlikely to account for these changes. Second, 16S rRNA sequencing provided taxonomic information but did not directly reveal microbial metabolic function. Integrated multi-omics profiling including metagenomics, metabolomics, and transcriptomics will be needed to clarify the functional pathways linking gut microbiota dysbiosis to neuroinflammation and depression-like behaviors. Third, although FMT supports the role of gut microbiota, the specific bacterial taxa and metabolites underlying the observed phenotypes remained to be determined. Fourth, Individual food intake, cumulative sucrose intake, and total energy intake were not continuously monitored; therefore, subtle differences in nutritional behavior and their potential contribution to gut microbiota alterations cannot be completely excluded. Finally, the present study did not identify an upstream neural signal specific to SI or a microbial pathway unique to PD. Moreover, individual housing in mice may not fully recapitulate human social isolation, as it primarily restricts direct social interaction while other sensory cues from conspecifics may remain.

Taken together, our findings are consistent with a mechanistic framework whereby SI aggravates depression-like behaviors in rotenone-induced PD mice through gut microbiota dysbiosis, intestinal-barrier dysfunction, neuroinflammatory responses, and disrupted microbiota-gut-brain axis signaling.

5. Conclusion

This study suggested that SI aggravated depression-like behaviors in rotenone-induced PD mice and that gut microbial dysbiosis contributed to this process through disruption of intestinal homeostasis, gut-barrier integrity, neuroinflammatory responses, and neurochemical regulation. These findings indicated that disruption of the microbiota-gut-brain axis may represent an important mechanism linking psychosocial stress to neuropsychiatric comorbidity in Parkinson's disease. Further studies are warranted to identify the specific microbial taxa, metabolites, and host signaling pathways involved, which may help guide the development of microbiota-targeted strategies for vulnerable patients with Parkinson's disease.

Abbreviations

PD, Parkinson's disease; SI, social isolation; FMT, fecal microbiota transplantation; TH, tyrosine hydroxylase; 5-HT, 5-hydroxytryptamine; BDNF, brain-derived neurotrophic factor; PBS, phosphate-buffered saline; SPT, sucrose preference test; TST, tail suspension test; OFT, open field test; CORT, corticosterone; IL-1β, interleukin-1β; IL-6, interleukin-6; TNF-α, tumor necrosis factor-α; ZO-1, zonula occludens-1; qPCR, quantitative reverse transcription polymerase chain reaction; SDS-PAGE, sodium dodecyl sulfate-polyacrylamide gel electrophoresis; RIPA, radioimmunoprecipitation assay; EDTA, ethylenediaminetetraacetic acid; BCA, bicinchoninic acid; TBST, Tris-buffered saline with Tween 20; HRP, horseradish peroxidase; IgG, immunoglobulin G; ECL, enhanced chemiluminescence; BSA, bovine serum albumin; DAPI, 4′,6-diamidino-2-phenylindole; ELISA, enzyme-linked immunosorbent assay; OTU/OTUs, operational taxonomic unit(s); PCoA, principal coordinates analysis; LEfSe, linear discriminant analysis effect size; CFU, colony-forming units; SEM, standard error of the mean; ANOVA, analysis of variance.

Availability of Data and Materials

The 16S rRNA gene sequencing data generated during the current study have been deposited in the NCBI Sequence Read Archive under BioProject accession number PRJNA1478958. Other datasets supporting the conclusions of this article are included within the article and its **Supplementary Material**. Additional datasets generated and/or analyzed during the current study are available from the corresponding author upon reasonable request.

Author Contributions

YX conducted animal experiments, performed statistical analyses and drafted the manuscript. YZ and WP participated in experimental data interpretation, critically revised the manuscript for important intellectual content. YW, MZ and XG conducted statistical analyses, helped in finalizing the figures and revised the manuscript. KZ and YY designed the studies and edited the manuscript. DG guided and supervised the whole experiment, critically reviewed and revised the manuscript for key intellectual content, and provided internal institutional support. All authors read and approved the final manuscript. All authors have participated sufficiently in the work and agreed to be accountable for all aspects of the work.

Ethics Approval and Consent to Participate

All animal experiments were approved by the Animal Ethics Committee of Xuzhou Medical University (Xuzhou, China; Approval No. 202309T002) and were carried out in accordance with the National Institutes of Health Guide for the Care and Use of Laboratory Animals and ARRIVE 2.0 (see **Supplementary Material**).

Acknowledgment

We thank Yongsheng Zhang, Xia Lan, and Menglu Zhou (Jiangsu Key Laboratory of Immunity and Metabolism, Department of Pathogen Biology and Immunology, Xuzhou Medical University) for their technical support.

Funding

This research received no external funding.

Conflicts of Interest

The authors declare no conflicts of interest.

Declaration of AI and AI-Assisted Technologies in the Writing Process

During the preparation of this manuscript, the authors used ChatGPT only to improve language readability. The authors reviewed and edited all AI-assisted outputs and take full responsibility for the final content.

Supplementary Material

Supplementary material associated with this article can be found, in the online version, at https://doi.org/10.31083/JIN55300.

References

[1] Zhu J, Cui Y, Zhang J, Yan R, Su D, Zhao D, et al. Temporal trends in the prevalence of Parkinson's disease from 1980 to 2023: a systematic review and meta-analysis. Lancet Healthy Longev. 2024; 5: e464–e479. https://doi.org/10.1016/s2666-7568(24)00094-1

[2] Su D, Cui Y, He C, Yin P, Bai R, Zhu J, et al. Projections for prevalence of Parkinson's disease and its driving factors in 195 countries and territories to 2050: modelling study of Global Burden of Disease Study 2021. BMJ (Clinical Research Ed.). 2025; 388: e080952. https://doi.org/10.1136/bmj-2024-080952

[3] Haiyang Wang, Zhanhua Liang, Zhongrui Yan, Yiming Liu. Executive Dysfunction and Prefrontal Cortex Dysregulation in Early-Onset Parkinson's Disease: An fNIRS Study. Journal of Integrative Neuroscience. 2025; 24: 36989. https://doi.org/10.31083/JIN36989

[4] Cong S, Xiang C, Zhang S, Zhang T, Wang H, Cong S. Prevalence and clinical aspects of depression in Parkinson's disease: A systematic review and meta-analysis of 129 studies. Neuroscience and Biobehavioral Reviews. 2022; 141: 104749. https://doi.org/10.1016/j.neubiorev.2022.104749

[5] Ahn S, Springer K, Gibson JS. Social withdrawal in Parkinson's disease: A scoping review. Geriatric Nursing (New York, N.Y.). 2022; 48: 258–268. https://doi.org/10.1016/j.gerinurse.2022.10.010

[6] Cryan JF, Dinan TG. Mind-altering microorganisms: the impact of the gut microbiota on brain and behaviour. Nature Reviews Neuroscience. 2012; 13: 701–712. https://doi.org/10.1038/nrn3346

[7] Shen Y, Fan N, Ma SX, Cheng X, Yang X, Wang G. Gut Microbiota Dysbiosis: Pathogenesis, Diseases, Prevention, and Therapy. MedComm. 2025; 6: e70168. https://doi.org/10.1002/mco2.70168

[8] Zhang K, Fujita Y, Chang L, Qu Y, Pu Y, Wang S, et al. Abnormal composition of gut microbiota is associated with resilience versus susceptibility to inescapable electric stress. Translational Psychiatry. 2019; 9: 231. https://doi.org/10.1038/s41398-019-0571-x

[9] Musleh-Vega S, Ojeda J, Vidal PM. Gut Microbiota-Brain Axis as a Potential Modulator of Psychological Stress after Spinal Cord Injury. Biomedicines. 2022; 10: 847. https://doi.org/10.3390/biomedicines10040847

[10] Hazani R, Weller A, Turjeman S, Sharon E, Saleev N, Moadi L, et al. The social microbiome: Eubacterium links gut microbiota to prosocial behavior in stressed and naïve rats, a gut-brain axis study. Brain, Behavior, and Immunity. 2025; 129: 505–520. https://doi.org/10.1016/j.bbi.2025.06.023

[11] Yasuda Y, Tokumatsu T, Ueda C, Sakai M, Sasaki Y, Norikura T, et al. Ecklonia cava Polyphenols Have a Preventive Effect on Parkinson's Disease through the Activation of the Nrf2-ARE Pathway. Nutrients. 2024; 16: 2076. https://doi.org/10.3390/nu16132076

[12] Fang X, Liu S, Muhammad B, Zheng M, Ge X, Xu Y, et al. Gut microbiota dysbiosis contributes to α-synuclein-related pathology associated with C/EBPβ/AEP signaling activation in a mouse model of Parkinson's disease. Neural Regeneration Research. 2024; 19: 2081–2088. https://doi.org/10.4103/1673-5374.391191

[13] Thaiss CA, Itav S, Rothschild D, Meijer MT, Levy M, Moresi C, et al. Persistent microbiome alterations modulate the rate of post-dieting weight regain. Nature. 2016; 540: 544–551. https://doi.org/10.1038/nature20796

[14] Yang X, Zhou Y, Tan S, Tian X, Meng X, Li Y, et al. Alterations in gut microbiota contribute to cognitive deficits induced by chronic infection of Toxoplasma gondii. Brain, Behavior, and Immunity. 2024; 119: 394–407. https://doi.org/10.1016/j.bbi.2024.04.008

[15] Pan W, Zhao J, Wu J, Xu D, Meng X, Jiang P, et al. Dimethyl itaconate ameliorates cognitive impairment induced by a high-fat diet via the gut-brain axis in mice. Microbiome. 2023; 11: 30. https://doi.org/10.1186/s40168-023-01471-8

[16] Gong Y, Liu X, Zhang S, Tang X, Zou J, Suo X. Antibiotic Changes Host Susceptibility to Eimeria falciformis Infection Associated with Alteration of Gut Microbiota. Infection and Immunity. 2022; 90: e0022922. https://doi.org/10.1128/iai.00229-22

[17] Li Y, Luo ZY, Hu YY, Bi YW, Yang JM, Zou WJ, et al. The gut microbiota regulates autism-like behavior by mediating vitamin B6 homeostasis in EphB6-deficient mice. Microbiome. 2020; 8: 120. https://doi.org/10.1186/s40168-020-00884-z

[18] Liu MY, Yin CY, Zhu LJ, Zhu XH, Xu C, Luo CX, et al. Sucrose preference test for measurement of stress-induced anhedonia in mice. Nature Protocols. 2018; 13: 1686–1698. https://doi.org/10.1038/s41596-018-0011-z

[19] Kleinridders A, Cai W, Cappellucci L, Ghazarian A, Collins WR, Vienberg SG, et al. Insulin resistance in brain alters dopamine turnover and causes behavioral disorders. Proceedings of the National Academy of Sciences of the United States of America. 2015; 112: 3463–3468. https://doi.org/10.1073/pnas.1500877112

[20] Aygun H. Exendin-4 increases absence-like seizures and anxiety-depression-like behaviors in WAG/Rij rats. Epilepsy &

Behavior: E&B. 2021; 123: 108246. https://doi.org/10.1016/j.yebeh.2021.108246
[21] Hsiao EY, McBride SW, Hsien S, Sharon G, Hyde ER, McCue T, et al. Microbiota modulate behavioral and physiological abnormalities associated with neurodevelopmental disorders. Cell. 2013; 155: 1451–1463. https://doi.org/10.1016/j.cell.2013.11.024
[22] Gibney SM, McGuinness B, Prendergast C, Harkin A, Connor TJ. Poly I:C-induced activation of the immune response is accompanied by depression and anxiety-like behaviours, kynurenine pathway activation and reduced BDNF expression. Brain, Behavior, and Immunity. 2013; 28: 170–181. https://doi.org/10.1016/j.bbi.2012.11.010
[23] Shoval G, Shbiro L, Hershkovitz L, Hazut N, Zalsman G, Mechoulam R, et al. Prohedonic Effect of Cannabidiol in a Rat Model of Depression. Neuropsychobiology. 2016; 73: 123–129. https://doi.org/10.1159/000443890
[24] Zhang Y, Ju M, Chen S, Yang W, Cai Y, Yu X, et al. Migration of CD8 + TSCM cells into intestine via PPBP-CXCR2 axis increases host stress susceptibility by inhibiting gut microbiome-derived homovanillic acid. Nature Communications. 2025; 16: 10165. https://doi.org/10.1038/s41467-025-65112-4
[25] Nagarajan R, Zhang H, Lyu J, Kambali M, Wang M, Rudolph U. Intranasal Insulin Mitigates Memory Impairment and Neuroinflammation in a Mouse Model of Hippocampal Aging. Pharmacology Research & Perspectives. 2025; 13: e70186. https://doi.org/10.1002/prp2.70186
[26] Zhang H, Pan Y, Jiang Y, Chen M, Ma X, Yu X, et al. Akkermansia muciniphila ONE effectively ameliorates dextran sulfate sodium (DSS)-induced ulcerative colitis in mice. NPJ Science of Food. 2024; 8: 97. https://doi.org/10.1038/s41538-024-00339-x
[27] Sayed IM, Inouye K, Das S, Alexander LC. Isolation of RNA from the Murine Colonic Tissue and qRT-PCR for Inflammatory Cytokines. Bio Protoc. 2023; 13: e4634. https://doi.org/10.21769/BioProtoc.4634
[28] Shi H, Yu Y, Lin D, Zheng P, Zhang P, Hu M, et al. β-glucan attenuates cognitive impairment via the gut-brain axis in diet-induced obese mice. Microbiome. 2020; 8: 143. https://doi.org/10.1186/s40168-020-00920-y
[29] Desai MS, Seekatz AM, Koropatkin NM, Kamada N, Hickey CA, Wolter M, et al. A Dietary Fiber-Deprived Gut Microbiota Degrades the Colonic Mucus Barrier and Enhances Pathogen Susceptibility. Cell. 2016; 167: 1339–1353.e21. https://doi.org/10.1016/j.cell.2016.10.043
[30] Zhang S, Liu X, Xu H, Zhang W, Shi C, Wang M, et al. TGR5 is essential for protecting from chronic stress-induced learning and memory impairments in mice by modulating inflammation associated with the gut-brain axis. J Neuroinflammation. 2026; 23. https://doi.org/10.1186/s12974-026-03898-w
[31] Quast C, Pruesse E, Yilmaz P, Gerken J, Schweer T, Yarza P, et al. The SILVA ribosomal RNA gene database project: improved data processing and web-based tools. Nucleic Acids Research. 2013; 41: D590–D596. https://doi.org/10.1093/nar/gks1219
[32] Cheng Y, Tong Q, Yuan Y, Song X, Jiang W, Wang Y, et al. α-Synuclein induces prodromal symptoms of Parkinson's disease via activating TLR2/MyD88/NF-κB pathway in Schwann cells of vagus nerve in a rat model. Journal of Neuroinflammation. 2023; 20: 36. https://doi.org/10.1186/s12974-023-02720-1
[33] Subramanian I, Farahnik J, Mischley LK. Synergy of pandemics-social isolation is associated with worsened Parkinson severity and quality of life. NPJ Parkinson's Disease. 2020; 6: 28. https://doi.org/10.1038/s41531-020-00128-9
[34] Lu R, Zhang L, Wang H, Li M, Feng W, Zheng X. Echinacoside exerts antidepressant-like effects through enhancing BDNF-CREB pathway and inhibiting neuroinflammation via regulating microglia M1/M2 polarization and JAK1/STAT3 pathway. Frontiers in Pharmacology. 2023; 13: 993483. https://doi.org/10.3389/fphar.2022.993483
[35] Zhao Z, Ning J, Bao XQ, Shang M, Ma J, Li G, et al. Fecal microbiota transplantation protects rotenone-induced Parkinson's disease mice via suppressing inflammation mediated by the lipopolysaccharide-TLR4 signaling pathway through the microbiota-gut-brain axis. Microbiome. 2021; 9: 226. https://doi.org/10.1186/s40168-021-01107-9
[36] Li ZL, Ma HT, Wang M, Qian YH. Research trend of microbiota-gut-brain axis in Alzheimer's disease based on CiteSpace (2012-2021): A bibliometrics analysis of 608 articles. Frontiers in Aging Neuroscience. 2022; 14: 1036120. https://doi.org/10.3389/fnagi.2022.1036120
[37] Grigoryan GA, Pavlova IV, Zaichenko MI. Effects of Social Isolation on the Development of Anxiety and Depression-Like Behavior in Model Experiments in Animals. Neuroscience and Behavioral Physiology. 2022; 52: 722–738. https://doi.org/10.1007/s11055-022-01297-1
[38] Kocamer Şahin Ş, Aslan E. Inflammation as a Neurobiological Mechanism of Cognitive Impairment in Psychological Stress. Journal of Integrative Neuroscience. 2024; 23: 101. https://doi.org/10.31083/j.jin2305101
[39] van der Maden MM, Verbeek MM, Beckers M. Lactobacillaceae and Parkinson's disease: An apparent paradox. Journal of Parkinson's Disease. 2025; 15: 269–281. https://doi.org/10.1177/1877718X241312401
[40] Sekimori T, Fukunaga K, Oizumi H, Baba T, Totsune T, Takeda A, et al. FABP2 is Involved in Intestinal α-Synuclein Pathologies. Journal of Integrative Neuroscience. 2024; 23: 44. https://doi.org/10.31083/j.jin2302044
[41] Chen X, Wang Z, Yang W, Fu Y. Levodopa Improves Behavioral Deficits of Mice with Parkinson's Disease Symptoms via Curbing NLRP3 Inflammasome Activation and Enhancing Tyrosine Hydroxylase Levels in the Striatum and Substantia Nigra. Journal of Integrative Neuroscience. 2024; 23: 2. https://doi.org/10.31083/j.jin2301002
[42] Nishiwaki H, Ito M, Ishida T, Hamaguchi T, Maeda T, Kashihara K, et al. Meta-Analysis of Gut Dysbiosis in Parkinson's Disease. Movement Disorders: Official Journal of the Movement Disorder Society. 2020; 35: 1626–1635. https://doi.org/10.1002/mds.28119
[43] Romano S, Savva GM, Bedarf JR, Charles IG, Hildebrand F, Narbad A. Meta-analysis of the Parkinson's disease gut microbiome suggests alterations linked to intestinal inflammation. NPJ Parkinson's Disease. 2021; 7: 27. https://doi.org/10.1038/s41531-021-00156-z
[44] Bai F, You L, Lei H, Li X. Association between increased and decreased gut microbiota abundance and Parkinson's disease: A systematic review and subgroup meta-analysis. Experimental Gerontology. 2024; 191: 112444. https://doi.org/10.1016/j.exger.2024.112444
[45] Yang X, Qian Y, Xu S, Song Y, Xiao Q. Longitudinal Analysis of Fecal Microbiome and Pathologic Processes in a Rotenone Induced Mice Model of Parkinson's Disease. Frontiers in Aging Neuroscience. 2018; 9: 441. https://doi.org/10.3389/fnagi.2017.00441
[46] Bhattarai Y, Si J, Pu M, Ross OA, McLean PJ, Till L, et al. Role of gut microbiota in regulating gastrointestinal dysfunction and motor symptoms in a mouse model of Parkinson's disease. Gut Microbes. 2021; 13: 1866974. https://doi.org/10.1080/19490976.2020.1866974
[47] Boertien JM, Murtomäki K, Pereira PAB, van der Zee S, Mertsalmi TH, Levo R, et al. Fecal microbiome alterations in treatment-naive de novo Parkinson's disease. NPJ Parkinson's Disease. 2022; 8: 129. https://doi.org/10.1038/

s41531-022-00395-8
[48] Pavan S, Gorthi SP, Prabhu AN, Das B, Mutreja A, Vasudevan K, et al. Dysbiosis of the Beneficial Gut Bacteria in Patients with Parkinson's Disease from India. Annals of Indian Academy of Neurology. 2023; 26: 908–916. https://doi.org/10.4103/aian.aian_460_23
[49] Hu L, Ye W, Deng Q, Wang C, Luo J, Huang L, et al. Microbiome and Metabolite Analysis Insight into the Potential of Shrimp Head Hydrolysate to Alleviate Depression-like Behaviour in Growth-Period Mice Exposed to Chronic Stress. Nutrients. 2024; 16: 1953. https://doi.org/10.3390/nu16121953
[50] Feng Q, Chen WD, Wang YD. Gut Microbiota: An Integral Moderator in Health and Disease. Frontiers in Microbiology. 2018; 9: 151. https://doi.org/10.3389/fmicb.2018.00151
[51] Wu M, Tian T, Mao Q, Zou T, Zhou CJ, Xie J, et al. Associations between disordered gut microbiota and changes of neurotransmitters and short-chain fatty acids in depressed mice. Translational Psychiatry. 2020; 10: 350. https://doi.org/10.1038/s41398-020-01038-3
[52] Lv M, Wang Y, Qu P, Li S, Yu Z, Qin X, et al. A combination of cecum microbiome and metabolome in CUMS depressed rats reveals the antidepressant mechanism of traditional Chinese medicines: A case study of Xiaoyaosan. Journal of Ethnopharmacology. 2021; 276: 114167. https://doi.org/10.1016/j.jep.2021.114167
[53] Tyler Halverson, Kannayiram Alagiakrishnan. The Brain-Gut-Microbiome Axis Across the Life Continuum and the Role of Microbes in Maintaining the Balance of Health. Journal of Integrative Neuroscience. 2025; 24: 36616. https://doi.org/10.31083/JIN36616
[54] Johnson ME, Stringer A, Bobrovskaya L. Rotenone induces gastrointestinal pathology and microbiota alterations in a rat model of Parkinson's disease. Neurotoxicology. 2018; 65: 174–185. https://doi.org/10.1016/j.neuro.2018.02.013